IEEE Access
Multidisciplinary ⋮ Rapid Review ⋮ Open Access Journal

Received May 7, 2020, accepted May 14, 2020, date of publication May 18, 2020, date of current version June 5, 2020.

Digital Object Identifier 10.1109/ACCESS.2020.2995214

Takagi-Sugeno Fuzzy Model-Based Semi-Active Control for the Seat Suspension With an Electrorheological Damper

XIN TANG[1], (Member, IEEE), DONGHONG NING[2], (Member, IEEE), HAIPING DU[2], (Senior Member, IEEE), WEIHUA LI[3], (Member, IEEE), AND WEIJIA WEN[1,4]

[1]Guangzhou HKUST Fok Ying Tung Research Institute, Guangzhou 511458, China
[2]School of Electrical, Computer and Telecommunications Engineering, University of Wollongong, Wollongong, NSW 2522, Australia
[3]School of Mechanical, Materials, Mechatronic and Biomedical Engineering, University of Wollongong, Wollongong, NSW 2522, Australia
[4]Department of Physics, Hong Kong University of Science and Technology, Hong Kong

Corresponding authors: Xin Tang (xintang@ust.hk) and Donghong Ning (dning@uow.edu.au)

This work was supported in part by the China Postdoctoral Science Foundation under Grant 2019M662847, and in part by the Guangzhou Postdoctoral International Training Program.

ABSTRACT Numerous research studies have been performed to help develop advanced control algorithms for semi-active seat suspension. This paper experimentally investigates a state observer-based Takagi-Sugeno (T-S) fuzzy controller for a semi-active seat suspension by equipping an electrorheological (ER) damper. A new ER damper prototype is designed, assembled, and tested. Then, a T-S fuzzy model is established to describe the ER seat suspension, which can facilitate the H∞ controller design considering the multi-objective optimization. A state observer is established and integrated into the controller to estimate the state information for the T-S fuzzy model in real-time. Additionally, the experimental validation of the control algorithm is critical in the practical application. A seat suspension test rig is built to validate the effectiveness of the proposed controller. The presented control algorithm is evaluated by comparing the corresponding test results to those with a skyhook controller. The experimental results demonstrate that the proposed T-S fuzzy control method, compared to the traditional control method, can further improve the performance of an ER seat suspension system.

INDEX TERMS Seat suspension, semi-active control, electrorheological (ER) damper, Takagi-Sugeno (T-S) fuzzy model.

I. INTRODUCTION

Vehicle seat suspension is applied to support the driver and make a user's ride comfortable. It is widely known that the driver's riding comfort and health highly depend on the vibration transferred from the road profile [1]. So far, the use of active and semi-active devices are the two main methods used to improve the performance of a seat suspension. Although an active method performs better in reducing vibration, its application is limited by its potential instability and high power consumption [2]. In contrast, the semi-active suspension provides a desirable performance similar to that of active suspension without the requirement of high power consumption and expensive hardware [3]. Currently, two kinds of semi-active devices are most widely applied in shock absorption control: an electrorheological (ER) fluid damper and a magnetorheological (MR) fluid damper [4]. As a nonlinear component, the ER/MR damper exhibits high hysteresis and nonlinear behavior, which lead a dynamic performance that is hard to accurately predict. For the purpose of control, Gavin [5] presented an ER damper algebraic model that is convenient for control and feedback linearization applications. To better describe the hysteretic behavior of an ER damper, Hoppe *et al.* [6] applied the augmented Bouc-Wen model to build the model of an ER damper. This model can effective to mitigate adverse effects on control performance.

In recent years, the ER and MR semi-active seat suspensions and the related control strategies have been widely

The associate editor coordinating the review of this manuscript and approving it for publication was Jinquan Xu.

studied [7], [8]. Do *et al.* [9] presented a direct adaptive fuzzy controller with a damping force feedback for an MR damper. Shin and Choi [10] proposed a robust controller integrated with interval type-2 fuzzy logic and sliding mode control. The effectiveness of the controller was verified by simulation and experimentation. To improve the performance of the semi-active suspension, Yao *et al.* [11], and Fei and Xin [12] designed adaptive sliding mode controllers to overcome the nonlinearity of a semi-active system. Ning *et al.* [13] presented a Takagi-Sugeno (T-S) fuzzy control strategy for an active seat suspension system. The experimental results show that both the robustness and accuracy of the T-S fuzzy controller can be guaranteed to control the active system.

However, the earlier studies often assumed that the state of the controlled system can be obtained by measurement. In practice, not all state variables can be measured in real time. In particular, the evolutionary variable of the Bouc-Wen model is nearly unmeasurable while an ER damper is working: To estimate the vertical velocity of the seat suspension by integrating the acceleration directly would reduce the accuracy of the estimation result. These variables are difficult to obtain for a normal vehicle equipped with only accelerometers and displacement sensors. Therefore, a state observer needs to be considered in the controller design. To solve the unstable flux estimation problem, Xiao *et al.* [14] presented an adaptive sliding mode observer which employs a sigmoid function as switch function to estimate the grid-side state. In our previous work of [15], we designed a state observer for the T-S fuzzy controller so that it can be used for MR vehicle suspension in practical applications. It is also noted that if the vertical movement of the seat suspension is too large, a large braking acceleration might be generated by the dead zone of the suspension deflection. In the situation that both the acceleration is too high and the deflection is too large, it is difficult for a driver to operate the steering wheel and brake pedal with his/her hands and feet, which will seriously affect driving safety. Therefore, the ride comfort and seat suspension deflection should be considered simultaneously with a weighted trade-off, which means that a controller with multi-objective optimization is required. In [16], a multi-objective genetic algorithm fractional order proportional-integral-derivative (PID) control was proposed for MR-based seat suspension. However, no experiment was conducted in this work to verify the effectiveness of the multi-objective algorithm in practical application.

The existing studies have shown that different control algorithms have different advantages and result in different performances, and that the performance of a controlled system highly depends on the degree of the nonlinearity of the dynamic model and the choice of control algorithm. Furthermore, for the above controlmethods, whether proposed for seat suspension or vehicle suspension control, an algorithm that is capable of solving the high nonlinearity of ER damper has rarely been developed. In the work of [17], Du *et al.* presented a sub-optimal H_∞ controller of a seat suspension and driver body model using ER dampers. However, an experiment has not been conducted to illustrate the practical effectiveness of this controller, though a comprehensive numerical evaluation was performed.

To develop an advanced model-based controller that can be applied to practical application, this paper proposes a state observer-based Takagi-Sugeno fuzzy (OTSF) controller and provide the experimental validation. With this controller, the nonlinear dynamic characteristics of the ER damper can be adequately considered in the controller design, and the desired performance of the semi-active seat suspension can be realized for a practical system. In the design of the existing model-based fuzzy controller [18], the device's fuzzy model was determined by training the input-output data sets. Thus, the expert experience used in selecting appropriate fuzzy sets and fuzzy rules highly affects the accuracy of the model. However, in this paper, the approach of 'sector nonlinearity' will be applied to the establishment of the T-S fuzzy model to reduce the impact of expert experience. To improve the comprehensive effectiveness of this approach to seat suspension, we integrate the multi-object-optimized process into the H_∞ controller. The optimization considers the seat acceleration and suspension deflection with a suitable weighted trade-off and normalization. A state observer is further designed to estimate the state variables of the controller in real-time. In this study, the design method proposed in [19] is applied to build a state observer.

The structure of this paper is as follows. The design and dynamic testing of an ER damper is presented in section II. Section III demonstrates the T-S fuzzy modeling process and describes the state observer and H_∞ controller design. Section IV presents the test results of the controller including the experimental setup and the results from sinusoidal and random excitation. Finally, the conclusion is presented in section V.

II. DESIGN AND TEST OF AN ER DAMPER

A. STRUCTURE AND PROTOTYPE

An ER damper was designed and assembled based on the specifications of a seat suspension system. Fig. 1 shows the configuration and the picture of the ER damper. It consists of ER fluid, a casing, an air accumulator, and a piston head into which the electrodes are set. ER fluid is injected into the casing which is divided into lower and upper chambers by the piston head. Between the bottom block and the floating piston, an airtight chamber is filled with air and acts as an accumulator.

B. PHENOMENOLOGICAL MODEL AND PARAMETER IDENTIFICATION

The ER damper was tested by using a 12 kN servo-hydraulic testing system. The experimental setup is shown in Fig. 2. A sinusoidal wave with a single frequency of 2 Hz and an amplitude of 15 mm (±7.5 mm) was chosen to excite the system. The applied voltage to the ER damper was varied

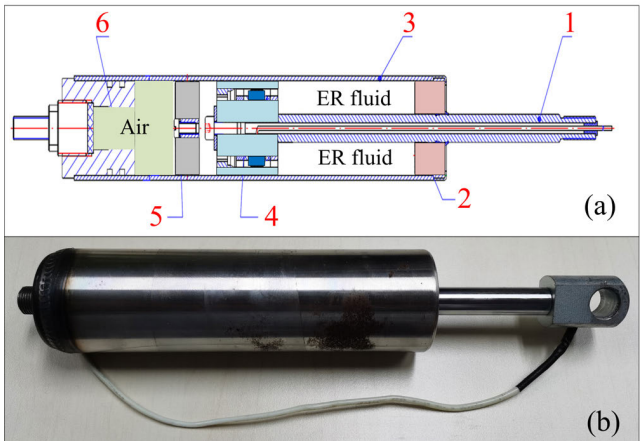

FIGURE 1. (a) Design of the ER damper (1. piston rod, 2. top cover, 3. casing, 4. electrode, 5. floating piston, 6. bottom block) and (b) photograph of a prototype.

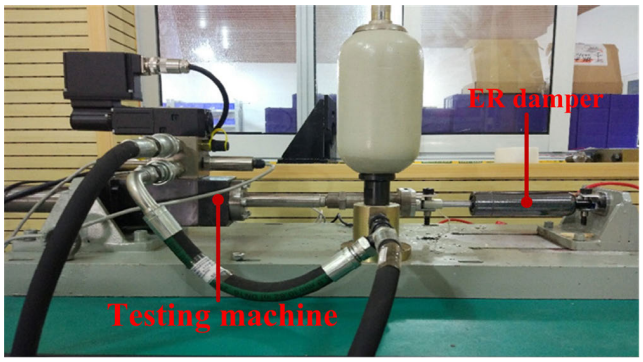

FIGURE 2. Testing system with the ER damper.

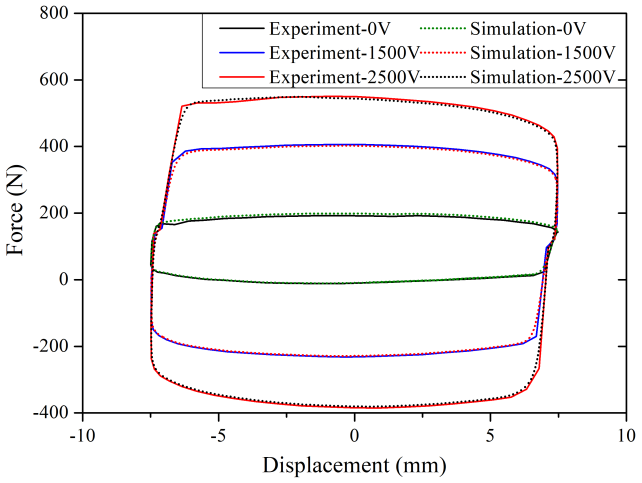

FIGURE 3. Measured response and fitting results.

TABLE 1. Parameter values of the ER damper.

Parameter	Value
A_e	456
β	1466400 m^{-2}
γ_e	2315698 m^{-2}
a_a	2584 N/m
a_b	7012 N/mV
c_{0a}	490 N·s/m
c_{0b}	1240 N·s/mV
k_0	398 N/m

from 0 V to 2500 V. The force and displacement data were measured and sent to a computer.

To date, the nonlinear characteristics of ER/MR dampers have been described by many different phenomenological models. Among these models, the Bouc-Wen model [20] is widely used for modeling hysteretic systems. The augmented Bouc-Wen model is capable of accurately describing the hysteretic behavior of an ER damper. However, in real-time control, there are many state variables that cannot be measured by sensors. In application, it is suggested that a simplified Bouc-Wen model that includes fewer measurable state variables is used. The model replaces some unmeasurable state variables from the original model while maintaining its accuracy to describe the hysteretic behavior of an ER device. The simplified Bouc-Wen model can be described as follows

$$\begin{aligned} F_{ER} &= c_0\dot{x}_e + k_0 x_e + a\,z, \\ \dot{z} &= -\gamma_e\,|\dot{x}_e|\,z\,|z| - \beta\dot{x}_e|z|^2 + A_e\dot{x}_e, \\ a &= a_a + a_b v, \\ c_0 &= c_{0a} + c_{0b} v, \\ \dot{v} &= -\eta\,(v - u), \end{aligned} \tag{1}$$

where

$$|z| = z \cdot \mathrm{sign}\,(z); \tag{2}$$

γ_e, β, and A_e are the parameters for adjusting the ER damper's hysteresis; a presents the evolutionary coefficient; c_0 is the viscous damping observed at higher velocities; k_0 presents the stiffness at high velocities; u is the control voltage sent to the power amplifier; v represents the output of a first-order filter; and x_e presents the relative displacement between the rod and the cylinder of the damper.

The parameters that fit the model of the ER damper were determined by the Simulink® parameter estimation function. These parameters are estimated by the program using the experimental results and the applied phenomenological model. In addition, the determined parameters are shown in Table 1. Fig. 3 shows the fitting results whose predicted hysteresis loops match well with the experimentally obtained data. For brevity, only the data under 3 different input voltages are illustrated in Fig. 3.

III. CONTROLLER DESIGN

The design process of the proposed controller is discussed in this section. In section III-A, a T-S fuzzy model for the semi-active seat suspension is established. In section III-B, a state observer is designed to estimate the state variables of the model in real-time. Then, an H_∞ controller that considers multi-object optimization is established in section III-C.

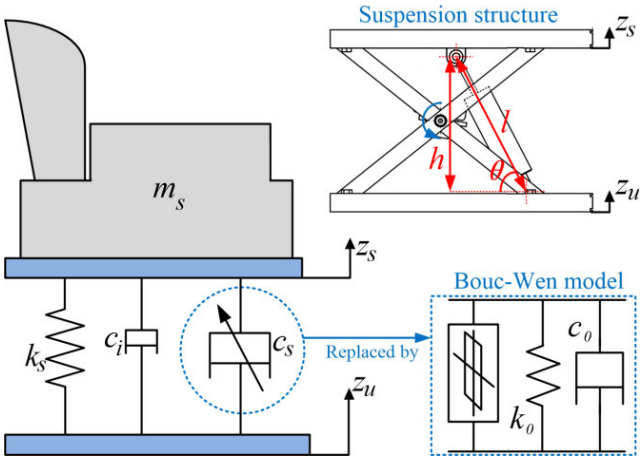

FIGURE 4. Model of the semi-active seat suspension.

A. T-S FUZZY MODELING OF SEAT SUSPENSION WITH THE ER DAMPER

The linear dynamic model of a seat suspension can be described by the following equation [21]:

$$m_s\ddot{z}_s = -k_s\left(z_s - z_u\right) - c_i\left(\dot{z}_s - \dot{z}_u\right) - c_s\left(\dot{z}_s - \dot{z}_u\right), \quad (3)$$

where m_s represents the mass of the seat and driver body; k_s denotes the spring constant of the seat suspension system; c_i represents the inherent damping of the seat suspension structure; c_s represents the damping force generated from a linear damper; and z_s and z_u are the displacements of the seat suspension system and the excitation from the vehicle cabin floor, respectively. It is noted that an inclined angle of the damper should be considered in the suspension structure. The kinematic model of the seat suspension is shown in Fig. 4, where θ is the damper's angle of inclination, which includes the initial installation angle and the one generated by the relative movement of suspension; h denotes the seat suspension height which includes the installation height and the relative movement of the seat suspension, $z_s - z_u$; and l is the length of the damper. With the movement of the seat suspension, the effective vertical output force of the damper can be described as $F_x = \sin(\theta)\cdot F$, where F is the actual output force of the damper and can be represented as

$$F = c_s\left[\left(\dot{z}_s - \dot{z}_u\right)/\sin(\theta)\right].$$

Therefore, the effective vertical damping force of the damper can be rewritten as $F_x = c_s\left(\dot{z}_s - \dot{z}_u\right)$.

To build the semi-active model, we can substitute the simplified Bouc-Wen model into the linear seat suspension model by replacing the linear damper model with the ER Bouc-Wen model. Fig. 4 demonstrates the semi-active model of ER seat suspension. Then, we can substitute (1) into (3) to obtain the dynamic equations of the ER seat suspension as follows

$$\begin{aligned} m_s\ddot{z}_s &= -c_r\left(\dot{z}_s - \dot{z}_u\right) - k_s\left(z_s - z_u\right) \\ &\quad - c_0\left(\dot{z}_s - \dot{z}_u\right) - k_0\left(z_s - z_u\right) - az, \\ \dot{z} &= -\gamma_e\left|\left(\dot{z}_s - \dot{z}_u\right)\right| z\,|z| - \beta\left(\dot{z}_s - \dot{z}_u\right)|z|^2 \\ &\quad + A_e\left(\dot{z}_s - \dot{z}_u\right), \\ a &= a_a + a_b v, \\ c_0 &= c_{0a} + c_{0b} v, \\ \dot{v} &= -\eta\left(v - u\right). \end{aligned} \quad (4)$$

Note that the term $c_s\left(\dot{z}_s - \dot{z}_u\right)$ in (3) is equivalent to F_{ER} in (1) and that the term $z_s - z_u$ in (3) is equivalent to x_e in (1). The semi-active suspension model can be tracked numerically in real-time control.

To establish the T-S fuzzy model, the state variables of the seat suspension model are defined as follows [22]:

$$x_1 = z_s - z_u, \quad x_2 = \dot{z}_s, \; x_3 = z, \; x_4 = v, \quad (5)$$

and the state vector is

$$x = \begin{bmatrix} x_1 & x_2 & x_3 & x_4 \end{bmatrix}^T, \quad (6)$$

and the output vector as the control voltage u, the disturbances is $w = \dot{z}_u$. Substituting (5) into (4), the system can be written as follows

$$\begin{aligned} \dot{x}_2 &= -\left(\frac{k_s}{m_s} + \frac{k_0}{m_s}\right)x_1 - \frac{1}{m_s}\left(c_r + c_{0a}\right)x_2 \\ &\quad - \frac{a_a}{m_s}x_3 - \left[\frac{c_{0b}}{m_s}\left(x_2 - w\right) + \frac{a_b}{m_s}x_3\right]x_4 \\ &\quad + \frac{1}{m_s}\left(c_r + c_{0a}\right)w, \\ \dot{x}_3 &= -|x_3|\left[\gamma_e\left|\left(x_2 - w\right)\right| - \beta\left(x_2 - w\right)sign\left(x_3\right)\right]x_3 \\ &\quad + A_e x_2 - A_e w, \\ \dot{x}_4 &= -\eta x_4 + \eta\, u. \end{aligned} \quad (7)$$

Then, we can define two fuzzy variables f_1 and f_2 as:

$$\begin{aligned} f_1 &= \frac{c_{0b}}{m_s}\left(x_2 - w\right) + \frac{a_b}{m_s}x_3, \\ f_2 &= |x_3|\left[\gamma_e\left|\left(x_2 - w\right)\right| - \beta\left(x_2 - w\right)sign\left(x_3\right)\right]. \end{aligned} \quad (8)$$

Then, equation (7) can be written as:

$$\begin{aligned} \dot{x}_2 &= -\left(\frac{k_s}{m_s} + \frac{k_0}{m_s}\right)x_1 - \frac{1}{m_s}\left(c_r + c_{0a}\right)x_2 \\ &\quad - \frac{a_a}{m_s}x_3 - f_1\cdot x_4 + \frac{1}{m_s}\left(c_r + c_{0a}\right)w, \\ \dot{x}_3 &= A_e x_2 - f_2\cdot x_3 - A_e w, \\ \dot{x}_4 &= -\eta x_4 + \eta\, u. \end{aligned} \quad (9)$$

We can describe the state-space of the semi-active seat suspension system as

$$\dot{x} = Ax + B_1 w + B_2 u, \quad (10)$$

where

$$A = \begin{bmatrix} 0 & 1 & 0 & 0 \\ -\left(\frac{k_s}{m_s} + \frac{k_0\sin(\theta)}{m_s}\right) & -\frac{\left(c_r + c_{0a}\right)}{m_s} & -\frac{a_a}{m_s} & -f_1 \\ 0 & A_e & -f_2 & 0 \\ 0 & 0 & 0 & -\eta \end{bmatrix},$$

$$B_1 = \begin{bmatrix} -1 & \frac{\left(c_r + c_{0a}\right)}{m_s} & -A_e & 0 \end{bmatrix}^T,$$

$$B_2 = \begin{bmatrix} 0 & 0 & 0 & \eta \end{bmatrix}^T.$$

To deal with the nonlinear system, the terms f_1x_4 and f_2x_3 in the T-S fuzzy model (9) should be replaced by linear subsystems. The variables f_1 and f_2 are limited in practical application by the vertical velocity and relative movement of the seat suspension, so that they can be represented as

$$\begin{aligned} f_1 &= M_1 f_{1max} + M_2 f_{1min}, \\ f_2 &= N_1 f_{2max} + N_2 f_{2min}, \end{aligned} \tag{11}$$

where M_1, M_2, N_1 and N_2 are fuzzy membership functions, and $M_1 + M_2 = 1$ and $N_1 + N_2 = 1$. $f_{\max}$ represents the upper bound of the nonlinearity of f; $f_{\min}$ is the lower bound. The four membership functions are defined as

$$\begin{aligned} M_1 &= \left(\frac{c_{0b}}{m_s}(x_2 - w) + \frac{a_b}{m_s}x_3 - f_{1min}\right) \\ &\quad / (f_{1max} - f_{1min}), \\ M_2 &= 1 - M_1, \\ N_1 &= \{|x_3|[\gamma |(x_2 - w)| - \beta (x_2 - w)\, sign\,(x_3)] - f_{2min}\} \\ &\quad / (f_{2max} - f_{2min}), \\ N_2 &= 1 - N_1. \end{aligned} \tag{12}$$

Thus, we can use the above linear subsystems to describe the nonlinear seat suspension system. The specific four possibilities can be presented as

$$\begin{aligned} &\text{IF } f_1 \text{ is } \mathrm{M_1} \text{ and } f_2 \text{ is } \mathrm{N_1} \text{ THEN } \dot{\mathrm{x}} = \mathrm{A_{(1)}x + B_1w + B_2}u, \\ &\text{IF } f_1 \text{ is } \mathrm{M_1} \text{ and } f_2 \text{ is } \mathrm{N_2} \text{THEN } \dot{\mathrm{x}} = \mathrm{A_{(2)}x + B_1w + B_2}u, \\ &\text{IF } f_1 \text{ is } \mathrm{M_2} \text{ and } f_2 \text{ is } \mathrm{N_1} \text{ THEN } \dot{\mathrm{x}} = \mathrm{A_{(3)}\,x + B_1w + B_2}u, \\ &\text{IF } f_1 \text{ is } \mathrm{M_2} \text{ and } f_2 \text{ is } \mathrm{N_2} \text{ THEN } \dot{\mathrm{x}} = \mathrm{A_{(4)}\,x + B_1w + B_2}u, \end{aligned} \tag{13}$$

where $A_{(i)}$ $(i = 1, 2, 3, 4)$. $(i = 1, 2, 3, 4)$ are obtained by replacing $f_{(i)}$ $(i = 1, 2)$ in the matrix A of (10) with $f_{(i)max}$ and $f_{(i)min}$, respectively. Then, the T-S fuzzy model (10) can be rewritten with the bounded state variables as follows:

$$\begin{aligned} \dot{x} &= \sum_{i=1}^{4} h_i \left[A_{(i)}\mathrm{x} + B_1 w + B_2 u\right] \\ &= A_h \mathrm{x} + B_1 w + B_2 u, \end{aligned} \tag{14}$$

where

$$\begin{aligned} A_h &= \sum_{i=1}^{4} h_i A_{(i)}, \\ h_1 &= M_1 N_1, \quad h_2 = M_1 N_2, \\ h_3 &= M_2 N_1, \quad h_4 = M_2 N_2, \end{aligned}$$

and $h_{(i)}$ $(i = 1, 2, 3, 4)$ satisfy: $\sum_{i=1}^{4} h_{(i)} = 1$.

B. STATE OBSERVER DESIGN

In the seat suspension system, the suspension deflection, $z_s - z_u$, can be measured by a displacement sensor; the seat acceleration, $\ddot{z}_s$, can be measured by an accelerometer. Thus, we can define the measurement variables as

$$\begin{aligned} Y &= \begin{bmatrix} z_s - z_u & \ddot{z}_s \end{bmatrix}^T \\ &= \sum_{i=1}^{4} h_i C_{1(i)} x \\ &= C_{1h} \cdot x, \end{aligned} \tag{15}$$

where

$$C_{1h} = \begin{bmatrix} 1 & 0 & 0 & 0 \\ -\left(\dfrac{k_s}{m_s} + \dfrac{k_0}{m_s}\right) & -\dfrac{(c_r + c_{0a})}{m_s} & -\dfrac{a_a}{m_s} & -f_{1h} \end{bmatrix}.$$

Based on the observer measurement in (15), the estimation error can be defined as

$$e = x - \hat{x}. \tag{16}$$

Then, the state observer can be derived by substituting the estimated state described in (16) into the system (14), and it can be represented as

$$\begin{aligned} \dot{\hat{\mathrm{x}}} &= \sum_{i=1}^{4} h_i \left[A_{(i)}\hat{x} + L_{(i)}\left(Y - \hat{Y}\right) + B_2 u\right] \\ &= A_h \hat{x} + L_h \left(Y - \hat{Y}\right) + B_2 u, \end{aligned} \tag{17}$$

where L are the state observer gains that need to be designed. Rearranging (17) gives

$$\dot{\hat{\mathrm{x}}} = (A_h - L_h C_{1h})\,\hat{x} + L_h Y + B_2 u. \tag{18}$$

To obtain the estimation error of the state space, we need to differentiate (16). Thus, the dynamic equation can be derived as

$$\begin{aligned} \dot{e} &= \dot{x} - \dot{\hat{\mathrm{x}}} \\ &= (A_h - L_h C_{1h})\, e + B_1 w. \end{aligned} \tag{19}$$

C. H∞ CONTROLLER DESIGN

This section describes the design of the H_∞ controller and the stability analysis of fuzzy systems based on a T-S state space model. With the application of the parallel distributed compensation scheme [23], the observer-based controller for the nonlinear system can be designed as

$$\begin{aligned} u &= \sum_{i=1}^{4} h_i K_{(i)} \hat{x} \\ &= K_h \hat{x}, \end{aligned} \tag{20}$$

where $K_{(i)}$ are the state feedback gains to be designed. Now, combine the estimated state vector and the error to obtain an augmented state vector

$$\bar{x} = \begin{bmatrix} \hat{x} & e \end{bmatrix}^T. \tag{21}$$

The augmented state space of (21) can be described as follows

$$\begin{aligned} \dot{\bar{\mathrm{x}}} &= \sum_{i=1}^{4} h_i \left(\overline{G}_{(i)}\bar{x} + \overline{B}_1 w\right) \\ &= \overline{G}_h \bar{x} + \overline{B}_1 w, \end{aligned} \tag{22}$$

where

$$\overline{G}_h = \begin{bmatrix} A_h + B_2K_h & -B_2K_h \\ 0 & A_h - L_hC_{1h} \end{bmatrix},$$

$$\overline{B}_1 = \begin{bmatrix} B_1^T & B_1^T \end{bmatrix}^T.$$

With regard to the multi-objective control, ride comfort and suspension deflection are often set as the main goal in a controller design. The controlled output $s$in this research can be described by suspension deflection and seat acceleration, $z_s - z_u$ and $\ddot{z}_s$, respectively; σ_1 and σ_2 are the values of the weighting parameters that should be set with the consideration of a suitable trade-off and normalization. Therefore, the optimized control output is defined as

$$\begin{aligned} s &= \begin{bmatrix} \sigma_1 (z_s - z_u) & \sigma_2 \ddot{z}_s \end{bmatrix}^T \\ &= \sum_{i=1}^{4} h_i \overline{C}_{2(i)} \overline{x} \\ &= \overline{C}_{2h} \overline{x}, \end{aligned} \tag{23}$$

where

$$\overline{C}_{2h} = \begin{bmatrix} \sigma_1 & 0 \\ -\sigma_2 \left(\dfrac{k_s}{m_s} + \dfrac{k_0}{m_s} \right) & -\sigma_2 \dfrac{(c_r + c_{0a})}{m_s} \\ \times \begin{matrix} 0 & 0 & 0_{1\times4} \\ -\sigma_2 \dfrac{a_a}{m_s} & -\sigma_2 f_{1h} & 0_{1\times4} \end{matrix} \end{bmatrix}.$$

Here, we choose the H_∞ norm as the performance measure to ensure that the controller has an appropriate response performance under different vibration excitation. The L_2 gain of the system (22) with (23) is defined as

$$\|T_{sw}\|_\infty = \sup_{\|w\|_2 \neq 0} \frac{\|s\|_2}{\|w\|_2}, \tag{24}$$

where $\|s\|_2^2 = \int_0^\infty s^T(t)\, s(t) \cdot dt$ and $\|w\|_2^2 = \int_0^\infty w^T(t)\, w(t) \cdot dt$.

To design the robust controller (20), we should guarantee that the closed-loop T-S fuzzy system (22) is quadratically stable. We can define a Lyapunov function for the system (22) as

$$\Pi(\overline{x}) = \overline{x}^T P \overline{x}, \tag{25}$$

where P is a positive definite matrix and $P = P^T$. By differentiating (25), we obtain

$$\dot{\Pi}(\overline{x}) = \dot{\overline{x}}^T P \overline{x} + \overline{x}^T P \dot{\overline{x}}. \tag{26}$$

Adding $s^T \mathrm{s} - \gamma^2 w^T w$ to the two sides of (26) yields

$$\begin{aligned} &\dot{\Pi}(\overline{x}) + s^T s - \gamma^2 w^T w \\ &\quad = \dot{\overline{x}}^T P \overline{x} + \overline{x}^T P \dot{\overline{x}} + s^T \mathrm{s} - \gamma^2 w^T w. \end{aligned} \tag{27}$$

Substituting (22) and (23) into (27) gives

$$\begin{aligned} &\dot{\Pi}(\overline{x}) + s^T s - \gamma^2 w^T w \\ &\quad = \left(\overline{G}_h \overline{x} + \overline{B}_1 w\right)^T P \overline{x} + \overline{x}^T P \left(\overline{G}_h \overline{x} + \overline{B}_1 w\right) \\ &\qquad + \left(\overline{C}_{2h} \overline{x}\right)^T \left(\overline{C}_{2h} \overline{x}\right) - \gamma^2 w^T w. \end{aligned} \tag{28}$$

Rearranging (28) gives

$$\begin{aligned} &\dot{\Pi}(\overline{x}) + s^T s - \gamma^2 w^T w \\ &\quad = \begin{bmatrix} \overline{x}^T \\ w^T \end{bmatrix}^T \begin{bmatrix} \overline{G}_h{}^T P + P\overline{G}_h + \overline{C}_{2h}^T \overline{C}_{2h} & P\overline{B}_1 \\ * & -\gamma^2 \end{bmatrix} \begin{bmatrix} \overline{x} \\ w \end{bmatrix}. \end{aligned} \tag{29}$$

Considering that

$$\Psi = \begin{bmatrix} \overline{G}_h{}^T P + P\overline{G}_h + \overline{C}_{2h}^T \overline{C}_{2h} & P\overline{B}_1 \\ * & -\gamma^2 \end{bmatrix}, \tag{30}$$

when the disturbance is zero, that is, $w = 0$, it can be inferred from (29) and (30) that if $\Psi < 0$, then $\dot{\Pi}(\overline{x}) < 0$, and the closed-loop fuzzy system (22) is quadratically stable. The equation (30) can be further rearranged to the linear matrix inequalities (LMIs) by applying Schur complement equivalence, as given below:

$$\begin{bmatrix} \overline{G}_h{}^T P + P\overline{G}_h & \overline{C}_{2h}^T & P\overline{B}_1 \\ * & -I & 0 \\ * & * & -\gamma^2 \end{bmatrix} < 0, \tag{31}$$

where I is a unit matrix.

To ensure the T-S fuzzy system (14) with the controller (20) is quadratically stable and for a given parameter $\gamma > 0$, the L_2 gain defined by (24) is less than γ, and the matrices $Q > 0$ and $Y > 0$, where $Q = P^{-1}$ and $Y = KQ$, should exist such that (31) is satisfied. Thus, the controller design can be regarded as a minimization of the performance measure parameter γ, which can be further described as

$$\begin{aligned} &\min\ \gamma^2 \\ &\textit{subject to}\ \text{LMIs (31)}. \end{aligned} \tag{32}$$

We can use common computing software such as MATLAB® to solve the LMIs in (31). The state feedback $\mathrm{K}_{(i)}$ matrix and the observer matrix $L_{(i)}$ can be determined after calculation. It is noted that the two matrices are the gains of the OTSF for real-time control. With the combination of the T-S fuzzy model and H_∞ technique, the proposed algorithm can directly control a nonlinear ER system. This method can effectively reduce the computational load of the controller and is easily implemented in practical application. After constructing the controller, the experimental validation work leaves aside the T-S fuzzy model and moves to the H_∞ controller in real-time.

IV. EFFECTIVENESS EVALUATION OF THE CONTROLLER

In this section, the proposed controller is evaluated on the test rig equipped with the semi-active seat suspension as described in section II. The seat suspension test rig for the experiment is described in section IV-A. Then, the designed

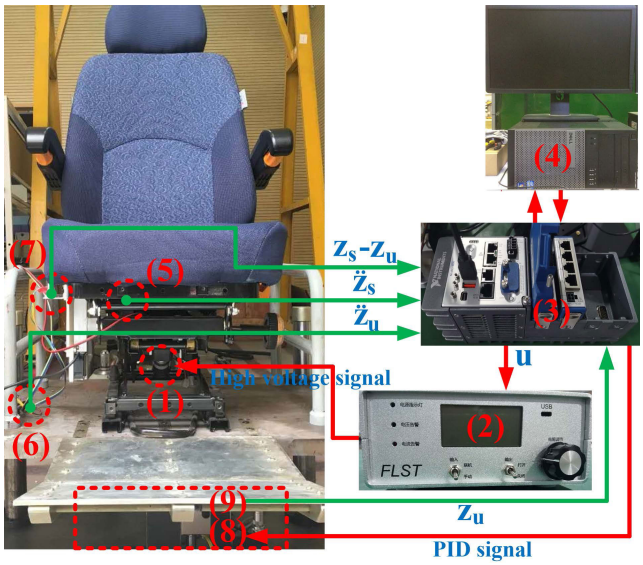

FIGURE 5. Test rig setup (1) the ER damper, (2) power amplifier, (3) NI real-time control board, (4) computer, (5-6) accelerometers, (7) laser sensor, (8) hydraulic actuator, and (9) actuator displacement sensor.

semi-active system is applied to the test rig and validated by sinusoidal excitation and random excitation profile in section IV-B and section IV-C, respectively.

A. EXPERIMENTAL SETUP

A seat suspension test rig is used to evaluate the proposed ER damper-based control algorithm. In the sinusoidal excitation test, we use a conventional passive seat suspension (Model: T803, Botai Corp.) as the comparison to the ER semi-active seat suspension controlled by OTSF. In the random excitation case, we conduct the passive ER seat suspension and the one with skyhook control as two comparisons for OTSF. Unlike the conventional passive seat suspension, the ER seat suspension use a semi-active damper instead of a passive one but with the same scissors structural frame.

The control schematic diagram of the test rig is described in Fig. 5. A hydraulic system manufactured by the China Shipbuilding Industry Group Corporation is applied to generate the external disturbance to the seat suspension. The hydraulic system is controlled by the control panel (model: cRIO-9030 CompactRIO, NI Corp.) with a PID algorithm. The imposed excitation z_u that acts as the external excitation is measured by a displacement sensor integrated into the hydraulic actuator and sent to the PID controller for real-time closed-loop control.

The primary parameters of the seat suspension system are selected as $k_s = 9550\,\mathrm{N/m}$, $c_r = 140\,\mathrm{N \cdot s/m}$, and $m_s = 72\,\mathrm{kg}$, which includes 55 kg as the driver mass.

The control system of the ER damper is a multi-input-single-output (MISO) system. One displacement signal, the suspension deflection, is measured by a laser sensor (model: LB-01, Keyence Corp.); and two acceleration input signals, the seat acceleration and the vibration excitation acceleration, are measured by the two accelerometers (model: ADXL327, Analog Devices Corp.). By running the control algorithm based on these inputs, the real-time control board (model: cRIO-9030 CompactRIO, NI Corp.) calculates the command voltage. It is noted that the input voltage required by the ER damper is limited in practice; the voltage range is often from 0 V to a positive value. Therefore, an asymmetric saturation of the control signal is taken into consideration. In this study, the control board calculates the command voltage u in the range 0-2.5 V, and sends the signal to the power amplifier (model: CMPXW-DC 24, FLST Corp.), which proportionally amplifies the command voltage to 0-2500 V. Then, the amplified voltage signal will act as the system input sent to the ER damper. After choosing the weighting factors $\sigma_1 = 1.4281$ and $\sigma_2 = 0.0363$ with suitable weighted trade-off and normalization, the control gain and state observer gain are calculated by the MATLAB® LMI Toolbox and obtained as

$$K_h = \begin{bmatrix} 5817 & 6502 & 2 & -13 \\ 5817 & 6502 & 2 & -13 \\ -5817 & -6502 & -2 & -13 \\ -5817 & -6502 & -2 & -13 \end{bmatrix},$$

$$L_h = \begin{bmatrix} 669 & 1244 \\ 669 & 1244 \\ -669 & -1244 \\ -669 & -1244 \end{bmatrix}.$$

B. SINUSOIDAL EXCITATION CASE

In the sinusoidal excitation test, a constant amplitude excitation is used. The excitation is designed with the frequency range of 1.0-3.0 Hz, which contains the sprung mass resonant frequency, with a step of 0.1 Hz. Here, the performance of the OTSF controller is evaluated by the vertical transmissibility of the seat. The transmissibility is taken as the ratio of $\ddot{z}_s$ to $\ddot{z}_u$ at any excitation frequency. Note that the acceleration transmissibility is calculated by using the RMS seat acceleration to divide the RMS vibration excitation acceleration.

The transmissibility results of the conventional passive seat suspension and the one controlled by OTSF under the sinusoidal sweep excitation is shown in Fig. 6. There is a

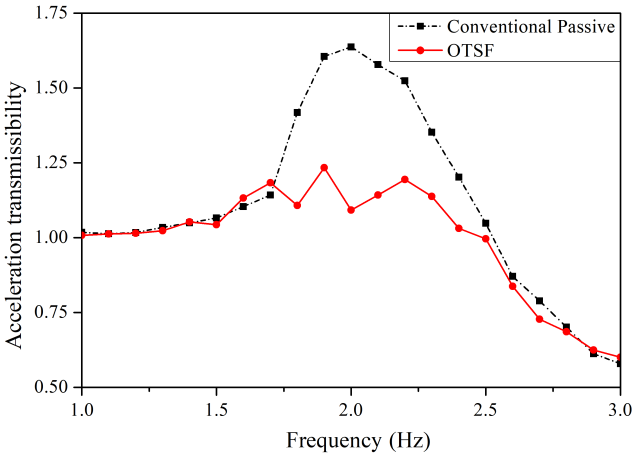

FIGURE 6. Acceleration response in the frequency domain.

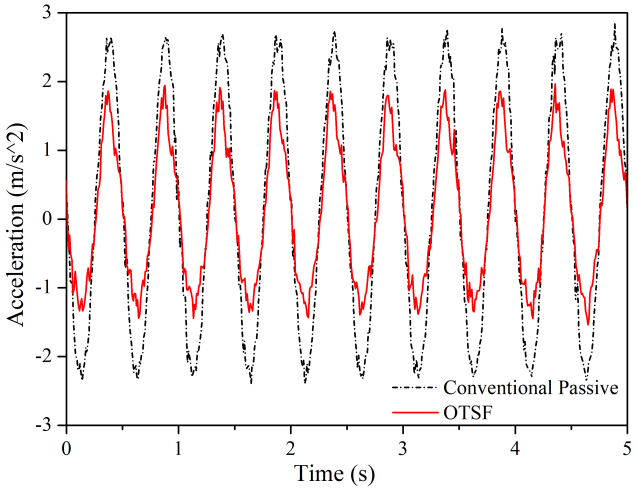

FIGURE 7. Seat acceleration under 2 Hz sinusoidal excitation.

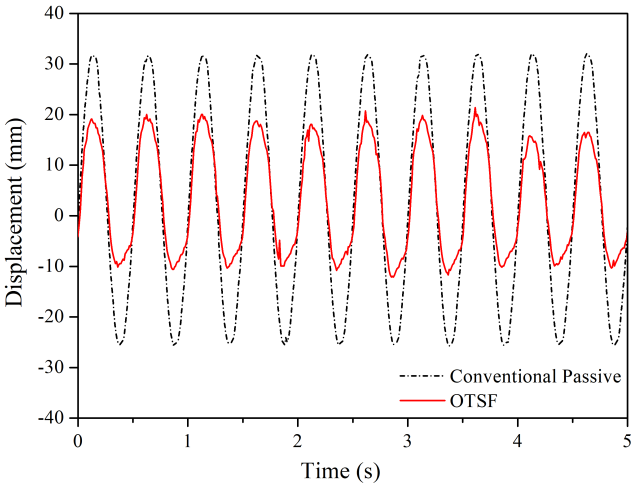

FIGURE 8. Suspension displacement under 2 Hz sinusoidal excitation.

peak value of the measured transmissibility, approximately 2 Hz, which is the resonance frequency of the suspension's sprung mass. The conventional passive seat suspension has difficulty reducing the acceleration transmissibility near that of the natural frequency of the sprung mass, since it is acting as a low-pass filter. As shown in Fig. 6, the controlled seat has an excellent performance in the tested frequency range.

To further compare the performance of the two seat suspensions, we plot the experimental results at 2 Hz in the time domain. The seat acceleration and suspension deflection responses are illustrated in Fig. 7 and Fig. 8, respectively. The controlled semi-active seat suspension performs much better than that the of conventional passive seat suspension in terms of both acceleration and suspension displacement. In particular, the maximum acceleration of the controlled suspension is $1.968\,\mathrm{m/s^2}$ and that the minimum acceleration is $-1.539\,\mathrm{m/s^2}$, so the peak-to-peak (PTP) value is $3.507\,\mathrm{m/s^2}$; the maximum acceleration of the conventional passive suspension is $2.839\,\mathrm{m/s^2}$, and the minimum acceleration is $-2.397\,\mathrm{m/s^2}$, so the PTP value is $5.236\,\mathrm{m/s^2}$. The PTP value reduction percentage of the controlled suspension compared with the conventional passive suspension is more than 33.02%.

Furthermore, the suspension deflections are compared, as shown in Fig. 8. the maximum displacement of the controlled seat is 21.39 mm and the minimum displacement is −12.14 mm, so the PTP value is 33.53 mm; the maximum displacement of the conventional passive seat is 32.14 mm, and the minimum displacement is −25.78 mm, so the PTP value is 57.92 mm. Therefore, the decrease in the PTP value of the controlled suspension compared with the conventional passive suspension is more than 42.1%. The corresponding PTP values are summarized in Table 2.

C. RANDOM EXCITATION CASE

A random excitation test is performed to evaluate the performance of the proposed controller. The random excitation

TABLE 2. PTP value under the sinusoidal excitation.

Objective	Conventional Passive	OTSF
Seat acceleration PTP ($\mathrm{m/s^2}$)	5.236	3.507
Reduction (%)	N/A	-33.02
Deflection PTP (mm)	57.92	33.53
Reduction (%)	N/A	-42.1

for the seat suspension is the vibration of the cabin floor generated by a quarter-car model under the class C random road profile in [24]. In this experiment, we ignore the interaction between the base of the seat suspension and the vehicle cab floor. Therefore, the sprung mass displacement of the quarter-car model is applied as the vibration input of the seat suspension.

The skyhook control [25] is generally considered as a reference control strategy to verify any new control strategies for semi-active control. To validate the performance of the OTSF, the skyhook controlled semi-active seat suspension and the one with no control (passive) are adopted for comparison. The skyhook controller defines the desired damping force as

$$F_{sky} = \begin{cases} c_{sky}\dot{z}_s & c_{sky}\dot{z}_s\,(\dot{z}_s - \dot{z}_u) > 0 \\ 0 & c_{sky}\dot{z}_s\,(\dot{z}_s - \dot{z}_u) \le 0, \end{cases} \tag{33}$$

where c_{sky} is the skyhook gain, which corresponds to the command voltage u_{sky} of 2500 V or 0 V.

The test results under random excitation are recorded and demonstrated in the time and frequency domains in Figs. 9-12, which show the results of seat acceleration, suspension deflection, and input voltage, respectively. In Fig. 9, the OTSF and the skyhook controller both have a better performance than the passive case, which has the greatest peak value during the whole time history. Comparing with

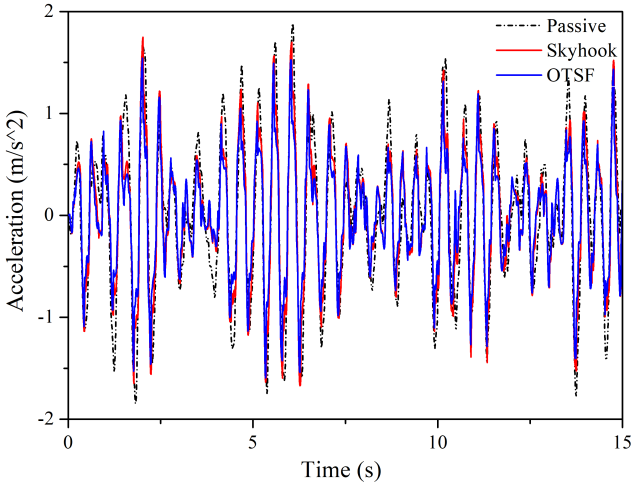

FIGURE 9. Seat acceleration under random excitation.

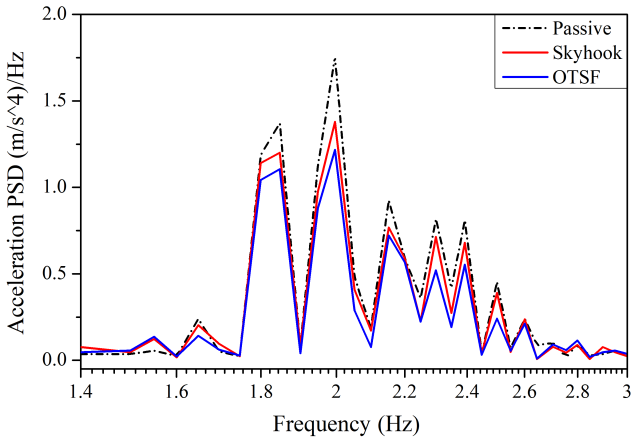

FIGURE 10. PSD of the seat acceleration.

TABLE 3. RMS value under the random excitation profile.

Objective	Passive	Skyhook	OTSF
Seat acceleration RMS (m/s^2)	0.546	0.482	0.448
Reduction (%)	N/A	-11.6	-17.9
Deflection RMS (mm)	5.517	4.278	3.921
Reduction (%)	N/A	-22.5	-28.9

the acceleration of the skyhook case, that of the OTSF case is further decreased.

The power spectral density (PSD) of seat acceleration is demonstrated in Fig. 10. It can be seen that the semi-active seat system has a peak value of approximately 2.0 Hz. The results further demonstrate that the OTSF controller has the best performance.

The system responses are summarized by the root-mean-square (RMS) values in Table 3 to further demonstrate the performance of the OTSF. In terms of both the acceleration and the deflection, the seat suspension controlled with

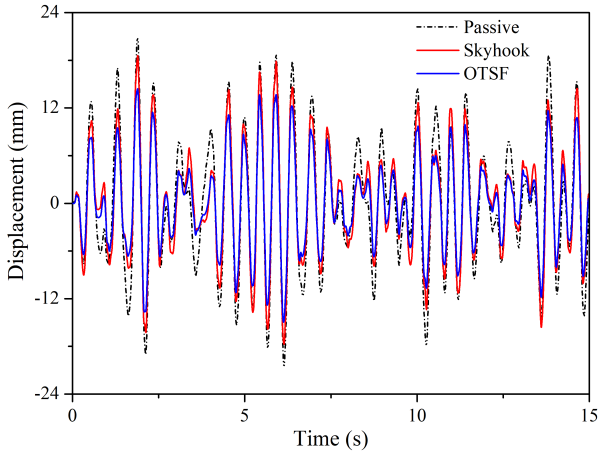

FIGURE 11. Suspension displacement under random excitation.

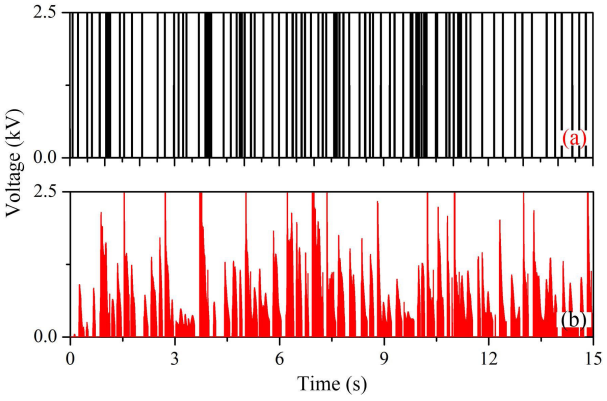

FIGURE 12. Input voltage under random excitation (a) skyhook and (b) OTSF.

OTSF has the smallest RMS value. In particular, the system with OTSF can reduce the RMS values of the acceleration and suspension deflection by approximately 17.9% and 28.9%, respectively, compared with the passive semi-active suspension. The reductions in the acceleration and suspension deflection of the OTSF are more effective than those of the typical skyhook control case (−11.6% and −22.5%). It can be inferred that the proposed controller provides a better performance than the traditional control algorithm for a random profile whose excitation has a wide frequency spectrum.

Fig. 12(a) and (b) demonstrates the input voltages of the skyhook control and the OTSF, respectively. The figure shows figure that the voltage signal obtained from the OTSF continuously varies. Contrary to those generated from the OTSF, the voltage signals generated from the skyhook controller are discrete values of either 0 V and 2.5 kV. It is noted that the applied current is low (at a microampere level), although the required highest voltage can reach 2.5kV [5]. Thus, the ER damper can be operated to ensure safety while using a low-power source.

V. CONCLUSION

In this paper, a state observer-based T-S fuzzy controller has been designed and investigated experimentally for a

semi-active seat suspension with an ER damper prototype. A T-S fuzzy model of the semi-active seat suspension has been proposed to cope with the nonlinearity of the ER damper and facilitate the controller design. In the practical application, only the acceleration and the suspension deflection are available for control feedback. Therefore, a state observer has been established to estimate the unknown state of the seat suspension in real-time. Based on the T-S fuzzy model, an H_∞ controller with multi-objective optimization has been designed to improve the overall performance of the seat suspension. In addition, a test rig has been constructed for the semi-active ER seat suspension system. Experimental validation under different excitations has been conducted to demonstrate the effectiveness of the proposed approach. The proposed controller and seat suspension can greatly benefit drivers by improving the working environment and protecting their safety and health.

REFERENCES

[1] G. S. Paddan and M. J. Griffin, "Effect of seating on exposures to whole-body vibration in vehicles," *J. Sound Vibrat.*, vol. 253, no. 1, pp. 215–241, May 2002.
[2] W. Sun, J. Li, Y. Zhao, and H. Gao, "Vibration control for active seat suspension systems via dynamic output feedback with limited frequency characteristic," *Mechatronics*, vol. 21, no. 1, pp. 250–260, Feb. 2011.
[3] D. Ning, S. Sun, J. Yu, M. Zheng, H. Du, N. Zhang, and W. Li, "A rotary variable admittance device and its application in vehicle seat suspension vibration control," *J. Franklin Inst.*, vol. 356, no. 14, pp. 7873–7895, Sep. 2019.
[4] G. Z. Yao, F. F. Yap, G. Chen, W. H. Li, and S. H. Yeo, "MR damper and its application for semi-active control of vehicle suspension system," *Mechatronics*, vol. 12, no. 7, pp. 963–973, Sep. 2002.
[5] H. P. Gavin, "Multi-duct ER dampers," *J. Intell. Mater. Syst. Struct.*, vol. 12, no. 5, pp. 353–366, May 2001.
[6] R. H. W. Hoppe, G. Mazurkevitch, U. Rettig, and O. Stryk, "Modelling, simulation, and control of electrorheological fluid devices," in *Lectures on Applied Mathematics*. Berlin, Germany: Springer, 2000, pp. 251–276.
[7] S.-B. Choi and Y.-M. Han, "Vibration control of electrorheological seat suspension with human-body model using sliding mode control," *J. Sound Vibrat.*, vol. 303, nos. 1–2, pp. 391–404, Jun. 2007.
[8] S. S. Sun, D. H. Ning, J. Yang, H. Du, S. W. Zhang, and W. H. Li, "A seat suspension with a rotary magnetorheological damper for heavy duty vehicles," *Smart Mater. Struct.*, vol. 25, no. 10, Sep. 2016, Art. no. 105032.
[9] X. P. Do, K. Shah, and S.-B. Choi, "Damping force tracking control of MR damper system using a new direct adaptive fuzzy controller," *Shock Vibrat.*, vol. 2015, pp. 1–16, Jul. 2015.
[10] D. Shin and S.-B. Choi, "Design of a new adaptive fuzzy controller and its application to vibration control of a vehicle seat installed with an MR damper," *Smart Mater. Struct.*, vol. 24, no. 8, pp. 85012–85031, Jul. 2015.
[11] J.-L. Yao, W.-K. Shi, J.-Q. Zheng, and H.-P. Zhou, "Development of a sliding mode controller for semi-active vehicle suspensions," *J. Vibrat. Control*, vol. 19, no. 8, pp. 1152–1160, Jun. 2013.
[12] J. Fei and M. Xin, "Robust adaptive sliding mode controller for semi-active vehicle suspension system," *Int. J. Innov. Comput., Inf. Control*, vol. 8, no. 1, pp. 691–700, Jan. 2012.
[13] D. Ning, S. Sun, F. Zhang, H. Du, W. Li, and B. Zhang, "Disturbance observer based Takagi-Sugeno fuzzy control for an active seat suspension," *Mech. Syst. Signal Process.*, vol. 93, no. 1, pp. 515–530, Sep. 2017.
[14] X. Xiao, Y. Zhang, X. Song, T. Yildirim, and F. Zhang, "Virtual flux direct power control for PWM rectifiers based on an adaptive sliding mode observer," *IEEE Trans. Ind. Appl.*, vol. 54, no. 5, pp. 5196–5205, Sep. 2018.
[15] X. Tang, H. Du, S. Sun, D. Ning, Z. Xing, and W. Li, "Takagi–Sugeno fuzzy control for semi-active vehicle suspension with a magnetorheological damper and experimental validation," *IEEE/ASME Trans. Mechatronics*, vol. 22, no. 1, pp. 291–300, Feb. 2017.
[16] S. Gad, H. Metered, A. Bassuiny, and A. A. Ghany, "Multi-objective genetic algorithm fractional-order PID controller for semi-active magnetorheologically damped seat suspension," *J. Vibrat. Control*, vol. 23, no. 8, pp. 1248–1266, May 2017.
[17] H. Du, W. Li, and N. Zhang, "Semi-active control of an integrated full-car suspension with seat suspension and driver body model using ER dampers," *Int. J. Veh. Des.*, vol. 63, nos. 2–3, pp. 159–184, Sep. 2013.
[18] H. Du and N. Zhang, "Model-based fuzzy control for buildings installed with magneto-rheological dampers," *J. Intell. Mater. Syst. Struct.*, vol. 20, no. 9, pp. 1091–1105, Apr. 2009.
[19] D. Ning, S. Sun, H. Li, H. Du, and W. Li, "Active control of an innovative seat suspension system with acceleration measurement based friction estimation," *J. Sound Vibrat.*, vol. 384, pp. 28–44, Dec. 2016.
[20] Y.-K. Wen, "Method for random vibration of hysteretic systems," *J. Eng. Mech. Division*, vol. 102, no. 2, pp. 249–263, 1976.
[21] D. Ning, H. Du, S. Sun, W. Li, N. Zhang, and M. Dong, "A novel electrical variable stiffness device for vehicle seat suspension control with mismatched disturbance compensation," *IEEE/ASME Trans. Mechatronics*, vol. 24, no. 5, pp. 2019–2030, Oct. 2019.
[22] D. Ning, H. Du, S. Sun, M. Zheng, W. Li, N. Zhang, and Z. Jia, "An electromagnetic variable stiffness device for semiactive seat suspension vibration control," *IEEE Trans. Ind. Electron.*, vol. 67, no. 8, pp. 6773–6784, Aug. 2020.
[23] H. Du, J. Lam, K. C. Cheung, W. Li, and N. Zhang, "Direct voltage control of magnetorheological damper for vehicle suspensions," *Smart Mater. Struct.*, vol. 22, no. 10, Sep. 2013, Art. no. 105016.
[24] X. Tang, "Advanced suspension system using magnetorheological technology for vehicle vibration control," Ph.D. dissertation, Dept. Mech. Eng., Univ. Wollongong, Wollongong, NSW, Australia, 2018.
[25] S.-B. Choi, M.-H. Nam, and B.-K. Lee, "Vibration control of a MR seat damper for commercial vehicles," *J. Intell. Mater. Syst. Struct.*, vol. 11, no. 12, pp. 936–944, Dec. 2000.

XIN TANG (Member, IEEE) received the B.E. degree in automation engineering from the University of Electronic Science and Technology of China, Chengdu, China, in 2012, and the Ph.D. degree from the School of Mechanical, Material and Mechatronics, University of Wollongong, Wollongong, NSW, Australia, in 2018.

He is currently a Research Fellow with the HKUST Fok Ying Tung Research Institute. His research interests include vibration control of semi-active vehicle suspension utilizing electrorheological (ER) and magnetorheological (MR) technology, robust control applications, human-like algorithms to enhance decision-making modeling for local path planning, and trajectory tracking control.

DONGHONG NING (Member, IEEE) received the B.E. degree in agricultural mechanization and automation from the College of Mechanical and Electronic Engineering, North West Agriculture and Forestry University, Yangling, China, in 2012, and the Ph.D. degree from the University of Wollongong, Wollongong, NSW, Australia, in 2018.

His research interests include active and semi-active vibration control, multiple degrees of freedom vibration control, interconnected suspension, electromagnetic suspension, and mechanical-electrical networks.

HAIPING DU (Senior Member, IEEE) received the Ph.D. degree in mechanical design and theory from Shanghai Jiao Tong University, Shanghai, China, in 2002.

From 2002 to 2003, he was with The University of Hong Kong. From 2004 to 2005, he was a Postdoctoral Research Associate with the Imperial College London. From 2005 to 2009, he was a Research Fellow with the University of Technology, Sydney. He is currently a Professor with the School of Electrical, Computer and Telecommunications Engineering, University of Wollongong, Wollongong, NSW, Australia.

Dr. Du was a recipient of the Australian Endeavour Research Fellowship, in 2012. He is a Subject Editor of the *Journal of Franklin Institute*. He is an Associate Editor of the IEEE Control Systems Society Conference. He is an Editorial Board Member for some international journals, such as the *Journal of Sound and Vibration*, the *IMechE Journal of Systems and Control Engineering*, and the *Journal of Low Frequency Noise, Vibration and Active Control*. He is a Guest Editor of *IET Control Theory and Application*, *Mechatronics*, *Advances in Mechanical Engineering*, and so on.

WEIHUA LI (Member, IEEE) received the B.E. and M.E. degrees from the University of Science and Technology of China, Hefei, China, in 1992 and 1995, respectively, and the Ph.D. degree from Nanyang Technological University, Singapore, in 2001.

From 2001 to 2003, he was a Research Fellow with the School of Mechanical and Production Engineering, Nanyang Technological University. Since 2003, he has been an Academic Staff Member with the School of Mechanical, Materials and Mechatronic Engineering, University of Wollongong, Wollongong, NSW, Australia. He has published more than 350 technical articles in refereed international journals and conferences.

Dr. Li received the number of awards, including the JSPS Invitation Fellowship, in 2014, the Endeavour Research Fellowship, in 2011, and the Scientific Visits to China Program Awards. He serves as an associate editor or editorial board member for nine international journals.

WEIJIA WEN received the B.E. and M.E. degrees from Chongqing University, Chongqing, China, in 1992 and 1995, respectively, and the Ph.D. degree from the Institute of Physics, Chinese Academy of Sciences, China, in 1995.

From 1995 to 1999, he was a Research Fellow with the Hong Kong University of Science and Technology (HKUST), Hong Kong, and UCLA. Since 1999, he has been an Academic Staff Member with the Department of Physics, HKUST. He has published more than 400 articles in his major research fields, including more than 350 journal articles and 50 conference invited report. He have been published more than 300 SCI articles. His refereed journal articles have been cited more than 10,500 times resulting in an H-index of 52. His main research interests include soft condensed matter physics, electrorheological (ER) and magnetorheological (MR) fluids, field-induced pattern and structure transitions, micro- and nano-fluidic controlling, advanced functional materials, including microsphere and nanoparticle fabrications, thin film physics, band gap materials, metamaterials, and nonlinear optical materials.